5
E-Beam Nanolithography Integrated with Scanning Electron Microscope

Joe Nabity, Lesely Anglin Campbell, Mo Zhu, and Weilie Zhou

1. Introduction

1.1. Basics of Microscope-Based Lithography

Electron beams have been used for lithography for decades [1,2] and a lithography system can easily be added to nearly all modern electron or ion microscopes, including scanning electron microscope (SEM), scanning transmission electron microscope (STEM), focused ion beam (FIB), and dual SEM/FIB microscope models. Nearly every microscope model will have inputs for external control of the XY beam position and most microscopes will have options for adding a fast beam blanker, which is an optional accessory for lithography. In most cases, the standard microscope stage will be used for lithography applications, and most stages can be controlled through a digital interface. Microscopes with a digital interface will also typically allow external control of column parameters, such as magnification, beam current, and focus as shown in Fig. 5.1.

A very important point is that adding a lithography system does not degrade or limit the functionality or performance of the microscope for imaging applications, because no customization of the microscope is typically required. Consequently, electron microscopes can become very versatile tools for micro and nano fabrication, since the same microscope used for the fabrication can also be used to view the resulting structures.

An SEM is the most common type of microscope used for lithography; however, nearly any system that allows external XY control of a point exposure can be used. Work with scanning tunneling microscope (STM) and atomic force microscope (AFM) lithography has been done [3,4]; however, these microscopes have not been widely used for lithography. In recent years, dual electron and ion beam microscopes have started to become more common for lithography, because a single lithography system can control either the e-beam or the ion beam, thus providing more fabrication capabilities than a single beam system.

1.1.1. Electron Source

There are two classifications for the sources in electron microscopes: (1) conventional sources use either tungsten hairpin filaments or lanthanum hexaboride (LaB_6) single crystal tips; and (2) field emission (FE) sources use either a cold cathode or a Schottky emitter (see Chapter 1). The latter is also known as a thermal FE source. Because of the lower cost, microscopes with conventional sources have traditionally been the models most widely used for lithography; however, microscopes with thermal FE sources provide both better imaging and better lithography.

When selecting between the two types of conventional sources for lithography, the main considerations are cost, convenience, brightness, and stability. The tungsten filaments have a lifetime of typically 40–200 h, while LaB_6 sources typically last significantly longer. Although the replacement cost for a tungsten filament is less than a LaB_6 source, the overall cost remains more or less the same. As LaB_6 source will have ~3 to 10× more current than a tungsten filament in the same spot size, lithography can be written faster; however, the stability of a LaB_6 source is ~3% per hour compared to ~1% per hour or better for tungsten. The ultimate lithography linewidths are basically the same for these sources; but a microscope with a LaB_6 source is easier to optimize because the higher brightness allows a higher beam current to be used, while a tungsten source will be more stable.

When selecting a cold cathode FE source vs. a thermal FE source for lithography as the primary application, the choice is simple. A thermal FE source will typically have a stability of ~1% over 3–10 h, while a cold FE source is inherently unstable and can change ±5% in minutes to ±20% or more per hour. Also, a cold FE source requires "flashing" periodically and the beam requires 1–2 h before becoming relatively stable and then typically becomes increasingly unstable as the vacuum in the gun degrades. While the imaging resolution of a cold FE source may be better than a thermal FE source, the instability of a cold FE source is a significant disadvantage for lithography applications. Even so, it can still be worthwhile to use a cold FE SEM for lithography when no other microscope is available. Table 5.1 shows the properties for different SEM electron sources.

1.1.2. Finest Linewidths

The finest linewidths achieved using conventional processing techniques with e-beam lithography typically range from ~10 to ~100 nm, where the microscope is the primary factor that determines the performance. The smaller linewidths are

TABLE 5.1. Comparing properties for common SEM electron sources

Property	Tungsten	LaB_6	Cold FE	Thermal FE
Source lifetime	40–300 h	1,000 h to 12 months	4–5 years	1–2 years
Imaging resolution (nm)	3.0–3.5	2.0–2.5	1.0	1.0–1.5
Max. probe current	0.1–10 uA	10 uA	2–10 nA	10–200 nA
Drift (%/h)	~1–2%	2–4%	~5–20%	0.05–1%

commonly produced with a 30 kV FE SEM, a 40 kV tungsten or LaB_6 SEM, or a ≥100 STEM, while low performance, low-cost SEMs may have a minimum feature size of 50–100 nm.

Besides the microscope performance, the main factors that determine the ultimate resolution are the choice of resist and substrate, accelerating voltage and beam current, writing field size, and the user's optimization of the microscope. These topics will be discussed in detail in the following sections.

1.1.3. SEM vs. Beam Writer

The typical SEM-based lithography system has many advantages over a dedicated electron beam writing system when research applications are the primary use. The advantages include cost, ease of use, maintenance, and versatility. A typical SEM can produce an accelerating voltage from ~200 eV to 30 kV, and can easily be changed as needed for different applications. Most microscopes can be successfully run by most graduate students after a reasonably short training period, and microscope service contracts generally keep a microscope running well with very little downtime. Commercial beam writers have the advantage when high volume and/or large area applications are required, since they have been specifically designed for such applications.

1.2. SEM Lithography System Considerations

1.2.1. Vector or Raster Writing

During normal image acquisition by an SEM, the beam is rastered from top to bottom of the full image area, where each line in the image is scanned from left to right. It is possible to do lithography with a similar raster if the beam can be blanked as needed as it scans across each raster line. However, the typical microscope-based lithography system uses a vector writing approach, where the beam moves in any direction and scans only the areas to be exposed. In a fully implemented vector writing system, the beam scan direction for sloped lines and circular arcs are along the line or arc and filled areas are not limited to simple XY scanning. In addition, for maximum flexibility, a microscope-based lithography system may provide two independent exposure point spacing parameters, where one will be along the line or arc that is being written, while the second will be in the perpendicular direction.

For a microscope-based lithography system, using a vector writing mode greatly increases the overall writing speed, since the exposed areas only need to be scanned. Using a vector writing mode can significantly reduce the demands on the beam blanker, since only two beam-on/beam-off events are needed for each pattern element. In contrast, a raster writing mode requires very precise blanking, especially when writing narrow lines perpendicular to the raster line scan direction.

A unique capability of the vector writing mode is that pattern writing can be accomplished even when the microscope does not have any blanker at all. This is possible, since the lithography system can jump the beam quickly enough between

pattern elements so that only an insignificant dose is applied to the path of the beam during the jump. Writing without a beam blanker is discussed in more detail below.

1.2.2. Writing Speed

Fundamentally, the overall writing speed for any direct write system depends on the beam current, sensitivity of the resist, and the maximum speed at which the beam can be moved across the exposure area. For most SEM systems, the beam current can be varied from ~10 pA to ~10 nA or more, and the current to be used must be selected based on the characteristics of the microscope. For example, some SEMs may write 50 nm lines with 1 nA of current while others may need to be run with less than 50 pA to achieve the same linewidths.

Most commercial microscope-based lithography systems have a maximum step rate for the beam of 3 MHz or higher. However, the typical microscope scan circuitry may be limited to a lower frequency. In general, if the lithography system is faster than the microscope scan coils, the ultimate writing speed will be limited by the materials, exposure conditions, and microscope, not the lithography system. In cases where pattern distortions are caused by the scan coils not "keeping up" with the lithography system, the solution is to reduce the beam current so that a slower writing speed can be used to provide the desired dose.

1.2.3. CAD Interface

A well-designed microscope-based lithography system will provide a powerful CAD program for pattern design. Also, when the GDSII and CIF formats are not the native format of the lithography system, support for importing patterns from these file formats will often be included, since these formats are standard for dedicated e-beam writing systems. In addition, microscope-based lithography systems will often include support for file exchange with DXF and DWG file formats, which are the formats used by AutoCAD and other general purpose CAD programs.

For the greatest flexibility, a microscope-based lithography system will allow ASCII pattern files to be created by any means. Some systems include a programming language that allows the users to write custom programs to automate any complex patterning requirements. For example, if a research application requires a structure to have a shape that is defined by a mathematical function, such as a logarithmic spiral, a programming language built into the CAD program can make it easy to create a custom function that produces the desired pattern in response to the parameters entered by the user.

1.2.4. Alignment

An advanced microscope-based lithography system provides both manual and fully automated alignment. The alignment is performed by imaging selected areas within the writing field and then registering the lithography coordinate system to marks on the sample. Generally, a 2×2 transformation matrix and XY offsets are

calculated based on the alignment results. Once calculated, these parameters are used to transform the exposure, so that the exposed pattern elements will be registered to the marks on the sample. Typical alignment accuracies range from 1:1,000 of the writing field to ~1:5,000, with accuracies down to ~20 nm being possible.

When a microscope-based lithography system includes a robust automated alignment feature, the system can use a standard automated microscope stage to get close to the desired location and then automatically align to much higher precision by scanning the registration marks. This allows "step-and-repeat" exposures to be processed with fully automated alignment at each field for tens, hundreds, or even thousands of fields, while using only the standard automated stage found on most modern SEMs.

1.3. SEM Connections

As stated earlier, almost any SEM, STEM, or FIB system can be used for lithography. The basic necessity is that the microscope must have analog inputs for external control of the beam position, where the typical input voltage range will be from ~±5 to ±10 V. Options for microscope-based lithography include an image signal output, a fast beam blanker, automated stage control, and a digital interface to the microscope.

Table 5.2 shows some of the more common electron microscope models that have been used for lithography. Other less common brands that have not been listed include Amray, Camscan, ISI, and Topcon. All models shown have the XY interface as a standard feature or available as an option.

1.3.1. Required: XY Interface and Beam Current Reading

Most modern microscopes have the required XY inputs either as standard or available as an extra cost option. For microscopes that do not have XY inputs, they can usually be added, if the schematics for the microscope are available. In this case, the basic procedure is to add relays to select between the internal scan generator and the external lithography system.

The only other required connection is for reading the beam current. Most microscopes have a single electrical connection to the specimen holder, which can be used to read the current that hits the sample. A Faraday cup can easily be made on most sample holders by drilling a blind hole ~2 mm wide, ~2 mm deep and covering it with a ~3 mm aperture with a 10–100 μm diameter hole. The aperture can be an inexpensive copper aperture or even a used SEM aperture.

A Faraday cup that inserts into the beam path either directly above the sample or higher in the column can be used, but is not required. An advantage of such a mechanism is that the current can be measured without moving the sample; however, care must be taken to ensure that the measured beam current in the cup is the same as the current measured at the sample. For example, a Faraday cup in the column may collect the primary beam and a significant current from stray electrons. In such a case, the excess current collected may be many times higher than the current measured at the sample.

TABLE 5.2. Comparing different models of SEMs

Brand	Models	Source	Blanker	Auto-Stage	Digital Interface
Cambridge	100—300 Series	W, LaB_6	Option or third party	Option or third party	None or serial
FEI/Philips	XL30 LaB_6	LaB_6	Option or third Party	Standard	Serial
FEI/Philips	XL30 FEG, SFEG, ESEM FEG, Sirion	tFE	Option^ or third party	Standard	Serial, Ethernet
FEI	Quanta	W	Option^ or third party	Standard	Ethernet
FEI	Quanta FEG, NanoSEM	tFE	Option^ or third party	Standard	Ethernet
FEI	Nova Nanolab	tFE/Ion	Option^ or third party	Standard	Ethernet
Hitachi	2000 and 3000 Series	W	Option or third party	Option or third party	None
Hitachi	4000 Series (not 4300SE)	cFE	Factory install or third party	Option	Serial
Hitachi	4300SE	tFE	Factory install	Option	Serial
JEOL	840,6300 and 6400	W,LaB_6	Option or third party	Option or third party	None serial
JEOL	5900, 6060, 6360, 6460, 6380, 6480	W,LaB_6	Third party	Option or standard	Ethernet
JEOL	6500F, 7000F	tFE	Third party	Standard	Ethernet
JEOL	6700F, 7400F	cFE	Third party	Standard	Ethernet
Leica/LEO	440, 1400	W,LaB_6	Option	Option	Serial
Tescan	Vega	W,LaB_6	Option	Option	Ethernet
Zeiss	Supra, Ultra,	tFE	Factory install^	Option	Serial
LEO	1500 Series				
Zeiss	EVO	W,LaB_6	Option	Option	Serial
LEO	440, 1400 Series				
Zeiss	1540 Crossbeam	tFE/Ion	Factory install^	Option	Serial

Notes:

1. In general, for older models the more expensive models within a series will give better lithography performance. For newer series, the beam quality is often virtually identical within a series, while other features will determine which models cost more. The microscope companies should always be contacted regarding details on current models, since features and options may change at any time.
2. Bold brand names are currently in business.
3. Usually, a tungsten (W) model may be upgraded to LaB_6. Once upgraded, either W or LaB_6 may be used.
4. "tFE" means thermal field emission. "cFE" means cold cathode field emission.
5. "Option" indicates that the microscope manufacturer has their own blanker or stage that is available as an option on a new microscope and may be available for retrofit of an existing microscope. For most new microscopes, an automated stage will be in the standard configuration, while an electrostatic blanker is rarely included as a standard feature. "^" indicates that the model includes a slow scan coil blanker as a standard feature, however, a fast electrostatic blanker is recommended for lithography use.
6. "Third party" indicates that a company other than the microscope manufacturer offers a compatible blanker or stage. In many cases, a third party blanker or stage will be offered as part of a new microscope purchase. For stages, third party automation packages are almost always available.
7. "Factory install" means that the blanker must be installed at the factory, which makes retrofitting the blanker to an existing microscope very expensive.

1.3.2. Optional: Image Signal

Nearly every microscope will have an image signal output that can be used by the lithography system for image acquisition. While it is not required to have an image signal for basic pattern writing, the image signal is required when the lithography system is used to align to existing marks on the sample. When an old analog microscope is used for lithography, the lithography system can often be used to acquire digital images. This capability will improve the functionality of an older microscope for imaging, in addition to allowing it to be used for lithography.

1.3.3. Optional: Beam Blanking

A microscope will ideally have a beam blanker that has a fast repetition rate, fast rise/fall times, and minimal on/off propagation delays. For most electron microscopes, such blankers are available either from the microscope manufacturer or from third-party vendors. Typical parameters for electrostatic blankers used for e-beam lithography are: repetition rate >1 MHz, rise/fall times <50 ns, and propagation delays <100 ns; however, slower blankers can still be useful. In general, an electrostatic blanker will be completely independent from the microscope user interface and be controlled directly by the lithography system with a TTL compatible on/off voltage.

While a fast beam blanker is certainly desirable for lithography, it is not required to have any blanker at all when using a vector writing system. When no blanker is available, the lithography system can jump the beam between pattern elements fast enough that a negligible dose is received along the path of the beam between the pattern elements. However, when no blanker is used, there are two main issues. One is that between pattern locations the beam will always be hitting the sample. Consequently, care must be taken to consider where the beam is hitting while the stage is being moved. The other is that when the beam is jumped between pattern elements, the scan coils will take some time to settle to the correct position after a long jump. This can result in distortions in the patterns at the starting point of each pattern element, if the beam has jumped a significant distance. In most SEMs, little to no distortion will be seen after a jump of 3–10 μm, but a significant distortion may be observed for longer jumps. A well-designed lithography system can allow the user to minimize the distortions by defining locations where the beam can settle, so that the lengths of the jumps to the desired pattern elements can be minimized. The settle areas will get a dose, however, a flexible lithography system will allow the user to select where the locations are, so that the functionality of the pattern being written will not be degraded.

When a microscope only has a slow beam blanker, the slow blanker can be used during stage moves between exposure fields. Many SEMs have a gun coil blanker that is a standard feature, which can be used this way if the microscope allows external control of the magnetic blanker.

1.3.4. Optional: Automated Stage

In general, having an automated stage for microscope-based lithography is not required. However, for most modern electron microscopes, the standard microscope stage will be automated and can be controlled through a digital interface, such as a serial or Ethernet connection. The advantages of using the standard microscope stage are that there is no additional expense and the versatility and functionality of the microscope are not degraded. Typically, a standard microscope stage will provide an absolute positioning accuracy of a few microns and an "over and back" repeatability of ~0.5–0.1 μm. When coupled with the alignment capability in a well-designed lithography system, a standard SEM stage can get close enough to the desired location for the lithography system to align accurately to marks on the sample.

When patterns must be "stitched" together without any imaging of registration marks in each field, a very accurate stage is required. In that case, most newer microscopes can be retrofitted with stages that use laser interferometer feedback to provide higher accuracy stage positioning. The disadvantages of such stages are that the cost is significant, i.e., around one half the cost of a new FE SEM and more than many W or LaB_6 models, and rotation, tilt, and often height adjustment will not be available.

1.3.5. Optional: Digital Interface

All newer SEM, STEM, and dual beam microscopes will have a digital interface for external control of the microscope parameters. The interface will typically be based on RS232 serial or Ethernet. A well-designed lithography system can take advantage of the digital interface and provide automated control of column parameters, such as magnification, focus, and beam current. Advanced control of microscope accelerating voltage can be possible, however, changing the kV typically requires the user to reoptimize the microscope, thus limiting the usefulness for fully automated control.

A well-designed microscope-based lithography system will also allow any executable to be automatically run at controlled points during the lithography processing, thus giving the user the ability to automate any function of the microscope that can be remotely controlled. For example, automated control of a gas handling system on a FIB microscope could be incorporated into a novel lithography application.

2. Materials and Processing Preparation

2.1. Substrates

Electron beam lithography is widely used to generate submicron or nanoscale structures and the choice of substrate is determined by the application. Normally, any solid substrate can be used with electron beam lithography, including

semiconductors (e.g., silicon, Ge, and GaAs), metals (e.g., Au, Al, and Ti), and insulators (e.g., SiO_2, PSG, and Si_3N_4). These materials can either be the substrates themselves or additive thin films on the substrates.

The electron beam lithography technique is most often employed to fabricate electronic or electro-related devices and structures, so silicon is currently the dominant substrate material for fabrication due to its inherent features: (a) well-characterized and readily available; (b) multitude of mature processing techniques available; and (c) intrinsic properties for electrical and electronic applications [5].

When electron beam lithography is performed on an insulating substrate, substrate charging may generate distortion overlay errors [6]. In addition, resist charging may prevent SEM inspection [7]. A simple solution to avoid pattern distortions from charging at high energies (~30 kV) is to deposit a thin layer of metal, such as gold, chrome, or aluminum, on the top of the resist. Electrons travel through the metal layer and expose the resist with reduced scattering [8]. After exposure, the metal layer is removed with the appropriate etchant before the development of the resist. A second method to provide charge dissipation is to coat a layer of conducting polymer under or over the resist [8–10]. Another approach is to apply a plasma process to the resist to increase its electrical conductivity by surface graphitization [11]. The advantage of this approach is its compatibility with industrial processes compared to the first two methods.

2.2. Resists

Electron beam resists are sensitive and are able to be developed by certain developers after exposure. The resists may produce either a positive or negative image compared to the exposed areas. Similar to photoresist, electron beam resists play two primary roles in lithography: (a) precise pattern transfer and (b) formation and protection of the covered substrate from etching or ion implantation [12]. The resists will normally be removed with the completion of these functions. However, in some cases the resists are also employed as a part of device and structure. Important properties of electron beam resists include resolution, sensitivity, etch resistance, and thermal stability [12], which are introduced in this section.

2.2.1. Resolution and Intrinsic Properties

In the process of electron beam lithography, the electrons will travel through the resist and lose energy by atomic collisions which are known as scattering. But, some of the electrons will be scattered back into the resist from the substrate. This phenomenon is known as backscattering. Scattering and backscattering will broaden lines scanned by the electron beam and will contribute to the total dose experienced by the resist.

The effects of scattering will vary with the electron beam energy. At low energies, electrons scatter readily, but travel only small distances after scattering. With higher energies, the scattering rate is lower, while the range after scattering

increases. Therefore, two approaches to high resolution can be obtained by high energy with a relatively low applied dosage or low energy with a relatively high applied dosage [13]. In either case, a very tightly focused beam is necessary to obtain small feature sizes.

Another issue for some electron beam lithography applications is the writing speed, which is primarily determined by the sensitivity of the resist and the magnitude of the current used during the writing. The highest resolution resists are usually the least sensitive [8].

The ultimate resolution of the resist is not set by electron scattering [14], but a combination of (a) the delocalization of the exposure process as determined by the range of the Coulomb interaction between the electrons and the resist molecules [15], (b) the straggling of secondary electrons into the resist [16], (c) the molecular structure of the resist, (d) the molecular dynamics of the development process (the tendency of the resists to swell in the developers), and (e) various aberrations in the electron optics. The resolution of resists is also influenced by the proximity effect, which is contributed by the adjacent features during the exposure. In some cases, this effect can significantly degrade exposure patterns which include a large number of closely spaced fine features, or small features placed near larger ones.

Mechanical and chemical properties such as etch resistance, thermal stability, adhesion, solid content, and viscosity are important to pattern transfer. Among these properties, the etch resistance is the most important when using the resist as an etch mask. Etch resistance specifies the ability of a resist to endure the etching procedure during the pattern transfer process. Another important property thermal stability meets the requirement for some specific process like dry etching [13]. As discussed before, e-beam resists are deposited on a variety of substrates including semiconductors (Si, Ge, GaAs), metals (Al, W, Ti), and insulators (SiO_2, Si_3N_4). Good adhesion is necessary to obtain good pattern transfer. Various techniques are used to increase the adhesion between resist and substrate including dehydration bakes before coating [12]: adhesion promoters such as hexamethyl-di-silazane (HMDS) and trimethylsilyldiethylamine (TMSDEA), vapor priming systems, and elevated temperature postbake cycles.

2.2.2. Positive Resists

For positive electron beam resists, the pattern exposed by the electron beam will be removed during development. These resists are usually high molecular-weight polymers in a liquid solvent, and undergo bond breakage or chain scission when exposed to electron bombardment. As a result, patterns of the positive resist exposed become more soluble in the developer solution.

Polymethyl methacrylate (PMMA) is one of the first resists developed for electron beam lithography and still the most commonly used low-cost positive electron beam resist. PMMA has high molecular weight, 50,000–2.2 million molecular weight (MW) (Nano PMMA and Copolymer, PMMA Resist Data Sheet, MicroChem Corp.), and exists in powder form dissolving in chlorobenzene, or the

safer solvent anisole. The thickness of the baked resist can be controlled by the coating speed and solid concentration. For example, PMMA (950,000 MW) with 3% concentration in chlorobenzene spun at 4,000 rpm will yield a thickness around 0.3 μm. The specific data for individual resists can be found in their material data sheets regarding different molecular weights, spin speed, concentration, and so on. The exposure dose for a typical electron acceleration voltage of 30 kV is in the range of 50–500 $\mu C/cm^2$ depending on the radiation source/equipment, developer, developing time, and pattern density. A common developer is a mixture of methyl isobutyl ketone (MIBK) and isopropyl alcohol (IPA). MIBK/IPA (1:3) is used for the highest resolution and MIBK/IPA (1:1) for the highest sensitivity. The developing time is typically 10–90 s depending on the applications.

The exposure process generates a natural undercut profile in the resists yielding a good geometry for the lift-off technique. More pronounced lift-off geometries may be achieved by using PMMA bilayers composed of two layer of PMMA with different molecular weight. The additional underlying layer of lower molecular weight PMMA requires a lower electron dosage for dissolution and thus gives more undercut. Even more extensive undercut may be achieved by replacing the lower PMMA with a layer of copolymer methyl methacrylate, P(MMA-MAA), or polydimethylglutarimide (PMGI), which are more sensitive to electron dosage. With very high electron dosages, PMMA will be cross-linked and insoluble in acetone, yielding a negative exposure process with acetone as the developer [17].

The ultimate resolution of PMMA has been demonstrated to be less than 10 nm [18]. However, PMMA has relatively poor sensitivity, poor dry etch resistance, and moderate thermal stability [19]. The assistance of the copolymer (PMMA-MAA) results in the better sensitivity image and thermal stability.

Another example of chain-scission resists is poly(1-butene sulfone) (PBS). PBS is a common positive resist for mask making due to its high sensitivity, around 3 $\mu C/cm^2$ at 10 kV [20]. However, PBS has poor etch resistance and needs tight control of processing temperature and humidity [21]. Poly(2,2,2-trifluoroethyl-α-chloroacrylate) (EBR-9) [22] is also used for mask making due to its long shelf life, lack of swelling in developer, and large process latitude [8].

ZEP is a new chain-scission positive resist developed on poly (methyl-α-chloroacrylate-co-α-methylstyrene) by Nippon Zeon Co. ZEP provides a high resolution and contrast comparable to PMMA but relatively low dose (8 $\mu C/cm^2$ at 10 kV). ZEP also has better etch resistance than PMMA.

The chemically amplified (CA) [23] resists have been developed recently for their high resolution, high sensitivity, high contrast, and good etch resistance [24–28]. Unlike the chain-scission process for PMMA during exposure, positive-tone CA resists are usually functionalized by the acid-catalyzed cleavage of labile blocking groups which protect the acidic functionalities of an inherently base-soluble polymer. Acid is generated in the exposed regions of the resist by radiation-sensitive photoacid generators (PAGs). As an example, a reported CA resist KRS containing a partially ketal-protected poly(*p*-hydroxystyrene) (PHS) has resolution less than 100 nm, sensitivity 12 $\mu C/cm^2$ at 50 kV, and contrast larger than 10 [20].

2.2.3. Negative Resists

Negative electron beam resists will form the reverse pattern as compared to positive resists. Polymer-based negative resists generate bonds or cross-links between polymer chains. The unexposed resists is dissolved during development while exposed resists remain, thus the negative image is formed.

Microposit SAL601 is a commonly used negative-tone chemically amplified electron beam resist with high sensitivity (6–9 $\mu C/cm^2$), good resolution (less than 0.1 μm), high contrast, and moderate dry etch selectivity (http://snf.stanford.edu/Process/Lithography/ebeamres.html). The main drawbacks of SAL601 are scumming and bridging between features, particularly in dense patterns, poor adhesion, and a very short shelf life.

An epoxy copolymer of glycidyl methacrylate and ethyl acrylate (COP) is another frequently used negative resist. COP shows very high sensitivities, 0.3 $\mu C/cm^2$ at 10 kV [8], because only one cross-link per molecule is sufficient to insolubilize the material. Although COP shows good thermal stability, its resolution is relatively poor, 1 μm, due to strong effect from the solvent swelling of the cross-linked region; and its plasma-etching resistance is also poor [29].

NEB-31 is a relatively new resist for electron beam lithography from Sumitomo Chemical, Inc. NEB-31 exhibits high resolution, 28 nm structures, high contrast, good thermal stability, good dry etch resistance, and long shelf-life [30].

Hydrogen silsesquioxane (HSQ) is a spin-on dielectric material for inter-metal dielectrics and shallow trench isolation in integrated circuit fabrication. Upon electron irradiation, inorganic 3D HSQ undergoes cross-linking via Si–H bond scission. This cross-linking results in an amorphous structure in HSQ similar to SiO_2 which is relatively insoluble in alkaline hydroxide developers [31]. HSQ has been employed as a negative resist for electron beam lithography, nanoimprint, and extreme ultraviolet (EUV) lithography [32–35]. As a competitive resist, HSQ has demonstrated high resolution, high contrast, moderate sensitivity, minimum line edge roughness, good etch resistance, high degree of mechanical stability [36,37], etc. A linewidth of about 7 nm with an aspect ratio of 10 has been reported for HSQ with 100 kV electron beam lithography. Dow Corning Corporation provides a series of commercial HSQ named as FOx®-1x and FOx®-2x [38].

Calixarene derivative is another example of high resolution negative resist. Although the dosage required is relatively high, ~20× as that of PMMA, calixarene derivatives are able to generate under 10 nm structures with little side roughness and high durability to halide plasma etching [39]. Calixarene also works with low energy: an optimal resolution (10 nm) at 2 keV is obtained with a reduced electron dose compared to high energy exposure [40].

SU-8 is a chemically amplified epoxy-based negative resist. Due to its good chemical and mechanical properties, SU-8 is normally employed to fabricate high aspect ratio 3D structures and serve as a permanent part of the device with the LIGA (a German acronym that stands for deep-etch x-ray lithography, electroplating, and molding) technique. As an electron beam resist, SU-8 is able to generate sub 50 nm structures with 0.03 nC/cm electron dose [41].

Most photoresists can be exposed by electron beam, although the chemistry is quite different from that of UV exposure [8]. Shipley UV-5 (positive) and UVN-2 (negative) are popular choices for their good resolution and excellent tech resistance.

2.2.4. Other Resists

In addition to the resists mentioned above, a number of metal halide resists are employed to achieve extremely high resolution, including LiF, AlF_2, MgF_2, FeF_2, CoF_2, SrF_2, BaF_2, KCl, and NaCl. For example, LiF_2 has demonstrated a high resolution of under 10 nm with line dose of 200–800 nC/cm [42].

A number of nanoscale structures have been made using the carbonaceous or silicaceous contaminants as the electron beam resist. The contaminations can be deposited on the surface due to (a) oil in the vacuum pumps, (b) organic residue on the sample surface, or (c) delivery to the point of impact of the beam via a capillary needle. With the third method, direct delivery of vapor via a capillary, it is possible to maintain a constant writing rate [43]. Under all deposition conditions, the required electron dose is very high, 0.1–1 C/cm^2. The contamination can be easily cleaned by heating the substrate to about 100°C [8].

Self-assembled monolayers (SAMs) are also used as the resists in electron beam lithography to obtain a high resolution. Since the thickness of the SAM is in the order of 1–2 nm, the scattering effects are negligible in the SAM resists. The molecules composing the SAM can be divided into three different functional parts: a head group that strongly binds to a substrate, a tail group that forms the outer surface of the monolayer, and a spacer linking head and tail [44]. However, the SAM resists demonstrate poor wet or dry etch resistance [45].

2.3. Spin Coating

The electron beam resists are normally applied to the substrates by the spin coating technique. A typical spin coating procedure typically involves (a) a dispense step (static or dynamic), and (b) spinning the substrate at high speed. Static dispense is to deposit a small amount of resists on the center of the substrate while stationary, and dynamic dispense is to apply the resists to the rotating substrate at low speed. Static dispense is simple, while dynamic dispense is more effective. After the dispense step, the substrates are accelerated to the final spin speed quickly. A high ramping rate generates better film uniformities than a low one [12]. Given a certain resist and substrate, the resist thickness after spin coating is determined by the spinning parameters including spin speed, spin time, etc. A separate drying step is generally needed after spin coating to further dry the film and improve the adhesion.

3. Pattern Generation

The complete pattern generation process extends from the initial concept for the pattern to the actual writing with the microscope. While the pattern design is relatively straightforward using a CAD interface to define the shapes, sizes, and

positions of the pattern elements, there are certain limitations of the writing system that should be considered during the layout. In addition to the design, there are a number of microscope parameters that need to be adjusted in order to properly configure the system such as working distance, accelerating voltage, and beam current or spot size. The final step before writing is to set up the microscope correctly by proper optimization and sample placement.

3.1. Design Guidelines

Using a design program, most commonly a CAD type, any shape can be constructed and interfaced with the writing software. As previously discussed, there are some constraints to the pattern design, such as the size of the writing field and the features themselves. It is also important to consider how the beam is actually exposing the resist and the limits that imposes. Another consideration while designing a pattern is the density of the features. As the beam exposes a region, secondary electrons can partially expose surrounding areas. This phenomenon is known as the proximity effect and is an important factor when writing high density patterns. A high density dot array, for example, will require a lower exposure dose than writing an individual dot or a low density array.

3.1.1. Field Size

Field size is one of the most important restrictions to pattern design, where the size of the writing field is determined by the magnification of the microscope. Fine features can usually be achieved with a writing field size of $50 \times 50\ \mu m^2$ to $200 \times 200\ \mu m^2$, depending on the type of microscope, where each microscope model will typically have certain magnification values that provide the best signal-to-noise ratio within the electronics of the microscope.

If a large area of fine features is desired, several fields can be positioned so that the field edges align with each other, which is commonly known as stitching. Unless care is taken, the edges of the pattern will mismatch due to irregularities in the stage movement. However, using alignment procedures as outlined in Section 1.2.4, these irregularities can be minimized to as little as 20 nm. Without the alignment, the mismatch can be as great as several microns. Depending on the purpose of the pattern this is often an acceptable amount of error.

3.1.2. Feature Size

Another important restriction to pattern design is the size of the features, which is limited by the resolution of the resist and the optimization of the microscope. Proper microscope optimization and a high resolution resist can routinely yield 50 nm features with most W or LaB_6 SEM models, while 20 nm and smaller are routinely produced with thermal FE SEMs.

3.1.3. Point Spacing

To obtain the best results from any lithography system, especially for demanding research applications, it is important to understand how the beam is moved to produce the pattern. To produce the finest lines, a single pass of the beam is typically used, which is composed of adjacent exposure points with a defined center-to-center distance. In this case, the center-to-center distance must be set to produce adequate overlap of the adjacent exposure points, which will typically be one fourth to half of the final linewidth. For wide lines or filled areas, a separately defined line spacing parameter will be used to control the spacing between adjacent passes of the beam.

In a sophisticated lithography system, the user will be able to independently adjust the center-to-center and line spacing parameters, while a more limited system will provide only a single parameter for both. Figure 5.1 shows a schematic of center-to-center distance and line spacing. An application that makes use of independent spacing is when the exposure points are intentionally defined to produce isolated dots in a rectangular array. Using this approach, the dots in the array will be the smallest dots that can be achieved given the system configuration and microscope setup.

3.2. System Configuration

In addition to the design of the pattern, there are system settings that need to be adjusted based on the application. Working distance can have an effect on many aspects of the writing process, such as spot size, interference, and magnification settings. Also, while considering design configurations and material properties, the accelerating voltage and current will be adjusted to define the beam for the intended application.

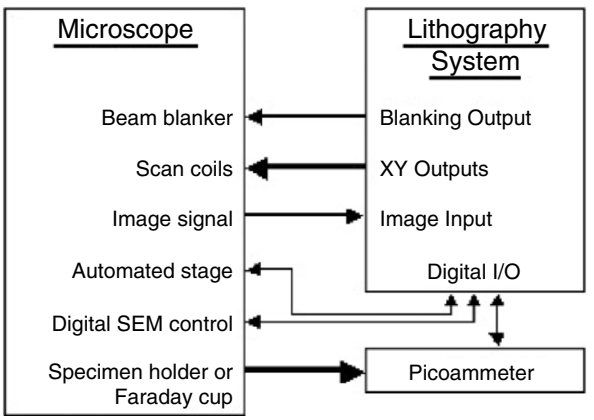

FIGURE 5.1. Bold arrows show required connections, medium arrows show typical connections, and thin arrows show optional connections.

The type of substrate and resist used will have an effect on the optimal exposure dose. For each type and molecular weight of a resist, the typical required dose will vary as shown in Table 5.1. A high Z substrate will have more backscattered and secondary electrons near the surface which will contribute to the overall dose affecting the resist.

3.2.1. Working Distance

The working distance influences the minimum spot size that is achievable; the susceptibility to external interference, and on some microscopes, the optimal magnification setting that should be used. A shorter working distance will improve the resolution of the microscope and will reduce the susceptibility of the beam to external interference. In cases where the microscope environment has magnetic fields, using a shorter working distance may have a dramatic effect on the writing quality. For most microscopes, a working distance between 5 and 10 mm is appropriate for writing fine features.

The working distance can also affect the optimal magnification settings. In all SEMs, the total magnification range will be divided into smaller ranges, where each range will use a different circuit within the microscope scan control electronics. When the scan control electronics change from one subrange to another, it will generally produce a small temporary image distortion and/or an audible click from a mechanical relay. The best signal-to-noise within the scan control electronics will be found at the higher magnification value after a transition. In some microscope models, the magnification values where the transitions occur depend both on the working distance and the accelerating voltage of the beam. For these models, it is often beneficial to use the same working distance for all fine lithography, so that the magnification value of the transition and the optimal magnification will not change.

3.2.2. Accelerating Voltage

Increasing the accelerating voltage will produce a greater electron penetration depth, thus lowering the number of scattered electrons in the resist, which will result in finer linewidths. The accelerating voltage can also affect the magnification settings in conjunction with the working distance previously mentioned. Most SEMs will have a maximum accelerating voltage of 30 kV, which will be the voltage used for most fine writing. When using an STEM, and accelerating voltage of 100 kV to ~300 kV may be used; however, these models typically allow only a very limited sample size, which reduces their versatility for lithography.

3.2.3. Beam Current (Spot Size)

A lower beam current will produce a smaller spot size on the sample than a larger beam current. The smallest spot size can be achieved by using the highest available accelerating voltage and a reasonably low beam current. The typical range

of beam current used for fine lithography is 5–50 pA, where the optimal value will vary depending on the model of SEM as well as the filament type. Some of the common ranges are: 5–10 pA for a W filament, 10–20 pA for a LaB_6 filament, and 20–50 pA for a FE microscope. In general, the goal is to use a beam current that is small enough to produce the desired feature sizes, but is also large enough to make the microscope reasonably easy to optimize.

3.3. Microscope Setup

Microscope setup is the final step before writing begins and it consists of two parts: microscope optimization and sample positioning. Fine lithography requires that the microscope be carefully optimized to ensure that the beam has the most favorable settings. The positioning of the sample affects the exposure positioning and axis alignment.

3.3.1. Microscope Optimization

Out of the settings that need to be optimized, focus and stigmatism are the most difficult adjustments to make for novice users. Thus, it is important to be familiar with the microscope and how to properly optimize for normal imaging before attempting to write patterns, where the optimization of the microscope is typically the easiest when using a gold resolution standard. Beginning with a low magnification, the focus and astigmatism should be alternately adjusted until a clear image can be achieved at a field size of approximately $1 \times 1\ \mu m^2$ or smaller. If a good image cannot be achieved, the adjustment technique and/or the microscope should be improved before attempting to write the smallest feature sizes. In addition, issues such as filament current, gun alignment, aperture centering (commonly referred to as "wobble"), and lens clearing (also known as hysteresis removal) should be addressed. Since these will depend on the specifics of the microscope model being optimized, it is beyond the scope of this chapter to provide a comprehensive procedure for all microscopes.

After the beam has been optimized on the gold resolution standard, the stage should be so that the surface of the resist is viewed on the edge of the sample away from the writing area. It is recommended to use the stage Z control to focus, since this will physically raise or lower the sample to the proper height without changing the settings of the microscope electronics. This technique removes the requirement that the gold resolution standard be at the same height as the writing surface. A final electronic focus adjustment can be done after the height has been adjusted, since by then only a small change should be necessary, which should not have any adverse effect on the beam optimization.

3.3.2. Sample Positioning

When first learning how to do lithography it is useful to write patterns near some obvious mark, such as a small, thin scratch made by a diamond scribe on the

substrate. Placing the pattern near the end the scratch will make the pattern easier to locate after development. Controlling the precise placement of a pattern in reference to other features is described in Section 1.2.4. Also, care must be taken when the patterns are placed far away from the last optimized location because the beam will become defocused if the stage motion significantly changes the height of the sample.

The orientation of the sample relative to the writing axes will affect the positions of the patterns on the sample, thus it is important to align the writing axes with and edge of the sample. This can be achieved by changing the rotation of the stage, adjusting the scan rotation, and/or using positioning features of the lithography software. When moving from one side of the writing sample to another, the vertical position should change less than 1 μm for every millimeter. Without this adjustment, patterns will be written with correct relative position to each other but without proper placement in relation to the sample.

4. Pattern Processing

After a pattern has been exposed in the resist, the subsequent processing will transfer the pattern either to the substrate or to a layer added after the lithography. The processing that is used will depend on the material system and the final structure that is desired. The sections below describe the common processing, as well as common problems that may be encountered. As with any multi-step lithography process, a failure in a later step will always be more significant than a failure in an early step, so avoiding problems becomes increasingly important.

4.1. Developing

During exposure, molecular bonds in the resist are created or broken depending on whether the resist is negative or positive, respectively. In either case, the developing agent dissolves the more soluble areas to produce the desired pattern. If the resist is left in the developer for too long, the less soluble resist areas will also dissolve; however, it is easy to have reasonably consistent results when the development time is on the order of a minute. In addition, the development rate will depend on the developer temperature, so maintaining a controlled developer temperature is recommended. The developer chemicals and development timing will depend on the type of resist used, however, the overall procedure is basically the same. After exposure, the resist-coated substrate is covered with a developing agent for a certain amount of time, rinsed, and dried, typically by blowing with dry N_2.

4.2. Coating and Liftoff

The two common methods of coating are sputtering and evaporation. A significant difference between sputtering and evaporation is the control over the direction of

the deposition material. In a typical sputtering system, the deposition is intended to strike the substrate with a wide range of incident angles, while evaporation is usually nearly collimated. This difference is significant because of the shape of the pattern cross section, as shown in Fig. 5.2. The shape is trapezoidal because of forward scattering of the incident beam and because some of the electrons scatter from the substrate and expose the bottom of the resist.

Liftoff is the process of removing the resist and the material that has been coated on top of the resist. The material that has adhered to the substrate will then be left, thus producing the desired pattern. The success of liftoff depends primarily on the adhesion of the coating to the substrate and whether or not the coating covers the sidewalls of the resist. Generally, an evaporated beam will be collimated enough to leave the sidewalls uncoated, while sputtering is much more likely to coat the sidewalls and make the liftoff step more difficult. For liftoff, it is important to know the thickness of the resist and to keep the coating thickness less than approximately two thirds of the resist thickness.

For PMMA, acetone is the solvent typically used during liftoff. The liftoff step with PMMA and acetone can be accomplished in many ways. In general, it is recommended to use the most gentle liftoff process that produces consistently good results. The simplest approach is to let the sample soak in room temperature acetone for about 20 min, or until it can be seen that the coating is floating off. Increasingly aggressive methods include using a squirt bottle, syringe, or ultrasonic cleaner to help remove the metal coating, or even to scrub the sample with a small brush. Heated acetone is sometimes used, however, this should only be done with the proper safety precautions.

4.2.1. Sputtering

In a plasma-magnetron sputtering system, the impact from ions from a plasma cause atoms from a metallic target to be ejected at all angles. The sputtered material coats the specimen which is placed below the target. The wide range of trajectories of the sputtered material is desirable for coating SEM specimens, since the metal will cover most surfaces and prevent charging during imaging. However, for lithography, it is generally undesirable to coat the sides of the resist walls that define the pattern, because this can cause ragged edges after liftoff or sections of the pattern may not lift off at all if the edges are coated with too thick of a layer. For larger patterns, having rough edges may not be a significant issue, however, having clean sidewalls becomes very important when doing liftoff with the very small features. Figure 5.3 shows a schematic representation of sputtering process and a cross section view of a pattern after sputtering has been done.

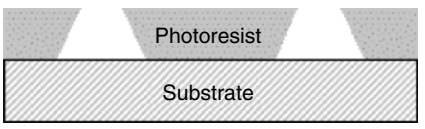

FIGURE 5.2. Schematic showing an undercut cross section of positive resist after exposure.

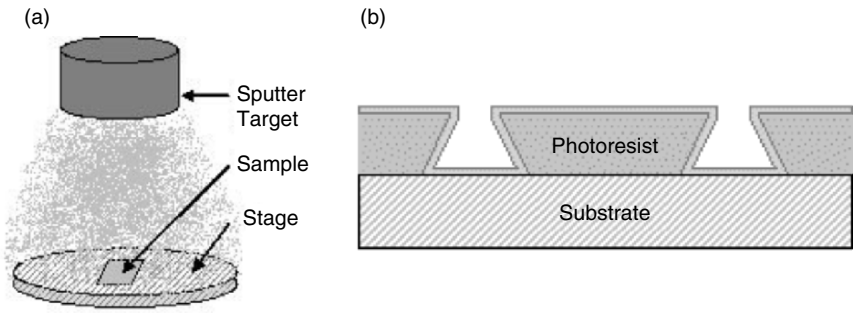

FIGURE 5.3. (a) Is a schematic representation of the sputtering process; and (b) shows a cross section view of a pattern after sputtering coating.

4.2.2. Evaporation

During thermal evaporation, the source material is placed in a boat or a filament coil, which is heated using an electrical current as shown in Fig. 5.4. Electron beam sputtering systems can also be used, which heat a localized spot in the source material using an electron beam. The sample can be placed either above or below the source material depending on the equipment being used. The evaporated material will be nearly collimated, so it is less likely to coat the sides of the pattern as compared to sputtering. This yields cleaner edges after removal of the resist, which is critical in high-resolution patterning. However, even with a collimated deposition, care must be taken to ensure that the deposited material hits at near normal incidence, otherwise the deposited material may coat some of

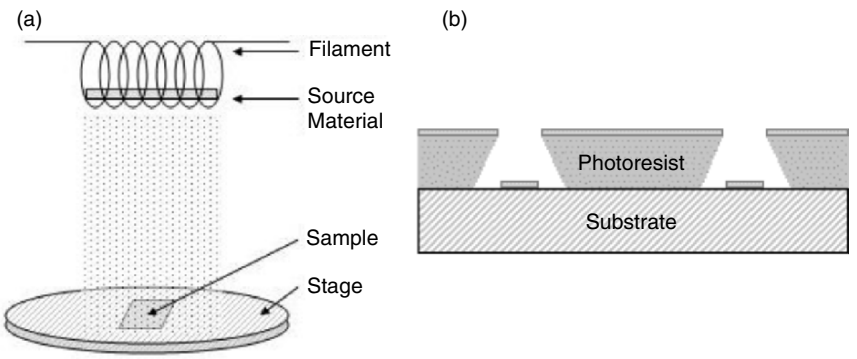

FIGURE 5.4. (a) Shows a schematic of a filament-style evaporation process; a boat is similar except that the sample is above the source material; and (b) shows a cross section view of the pattern after it has been coated using evaporation.

the sidewalls and/or may not reach the bottom of narrow features that have a high aspect ratio between the resist thickness and the feature size.

4.3. Etching

A variety of etching methods can be utilized, including wet chemical etching and reactive ion etching, and the etch may be isotropic or nonisotropic, depending on the method. In general, the resist will be used to protect parts of the substrate, while the exposed areas will be etched away. An important issue when etching is the relative etch rate of the substrate compared to the etch rate of the resist. In some cases when a resist cannot be used as an adequate etch mask, an extra layer will be used as the final etch mask, while the resist will be used to pattern the intermediate layer.

4.4. Pattern Checking and Common Errors

For beginners, it is useful to write a standard pattern on every sample, at least until consistently good results are obtained. The examples to follow are created using the same "wheel" pattern, which is a very effective diagnostic tool, because it allows pattern problems that are caused by poor focus and/or astigmatism in the beam to be easily identified.

4.4.1. Proper Writing

When a pattern is exposed correctly, lines should be straight with crisp edges and have a uniform thickness throughout. The final linewidth from a single line pass of the beam will depend primarily on the resist, beam focus/astigmatism during writing, and the applied line dose. An example of the wheel that has been done correctly is shown in Fig. 5.5. The slightly darker wedges inside of the "wheel" indicate that the area is becoming charged while viewing. This shows that the coating has not covered the sides of the pattern and will most likely lift off cleanly when the resist is removed.

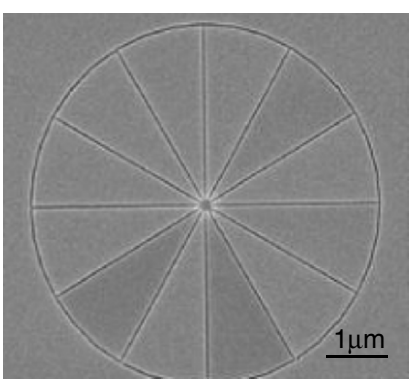

FIGURE 5.5. An example of the wheel pattern that has been written correctly.

4.4.2. Common Problems

Several types of errors can be determined by viewing a diagnostic pattern. Three of the most common errors during pattern generation are astigmatism in the beam, poor focus, and over- and underexposure. Typically, for new users pattern exposure problems are caused by a poor optimization of the beam, but the situation will improve as the user becomes better at running the microscope. Systematic problems, such as line noise, ineffective beam blanking, or general problems with the microscope itself, will usually have a distinctive effect on the outcome of the pattern.

Astigmatism is when the electron beam has an elongated cross section, represented as an oval in Fig. 5.6, as opposed to the ideal circular shape. As the beam moves from point to point forming a line in the direction of the long axis of the oval (vertical in Fig. 5.6a), all of the applied dose hits along the narrow path of the beam. However, when the beam steps in the direction of the short axis of the oval (horizontal in Fig. 5.6a), the dose is applied to a wider area along the line. This effect will produce a 90° asymmetry in the patterns, which is especially easy to identify in the wheel pattern. A schematic showing the dose distribution along the long axis and short axis directions is shown in Fig. 5.6a. An actual exposure of the wheel pattern written in PMMA is shown in Fig. 5.6b. In this case, the elongated beam lines up between the 5–11 o'clock and 6–12 o'clock spokes of the wheel, and the 90° asymmetry is very obvious. This is the classic sign of a pattern written with astigmatism in the beam.

When the beam is not well focused on the surface of the resist, large features will have only a small effect, where the radius on corners will be larger than expected. However, significant changes are caused when narrow lines are written with a beam that is out of focus. In general, poor focus will cause the applied dose for a narrow line to be spread over a larger area than desired. If the line dose is close to the critical dose for writing the smallest line, this broadening will effectively make the line underexposed. When the line dose is sufficiently above the

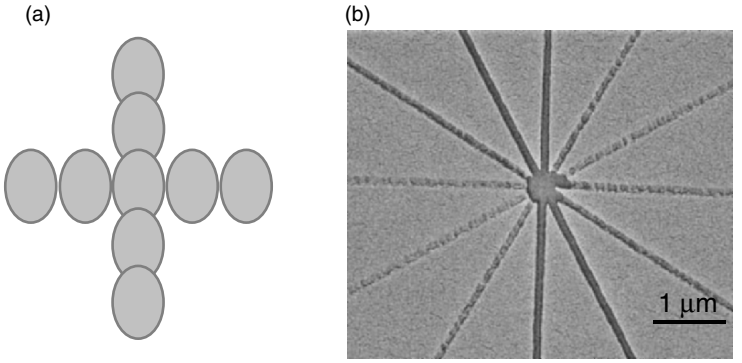

FIGURE 5.6. (a) Schematic showing how the shape of the beam affects the applied dose; and (b) the wheel pattern showing the effect of a beam with astigmatism.

critical dose, the broadening of the beam will make the exposed line larger than desired. In both cases, any junctions of single passes of the beam will effectively receive a double dose, and will generally appear to be "bloomed" out compared to the nearby lines. A picture of the wheel pattern that has been written in PMMA with a slightly degraded focus is shown in Figure 5.7. In this case, the lines of the pattern are slightly underexposed, while the junctions are overexposed. This is the classic sign of a poorly focused beam.

Overexposure causes patterns to become enlarged or in extreme cases a positive resist will receive enough dose to make it cross-link and develop like a negative resist. An image of an enlarged pattern and a positive/negative pattern is shown in Fig. 5.8. In this case, the center white dot is where the PMMA has become cross-linked due to the 12× dose where the 12 lines start at the center, and the entire central area has enlarged from the high dose. When the applied dose is too small, the lines of the resulting exposure will be shallow and/or discontinuous.

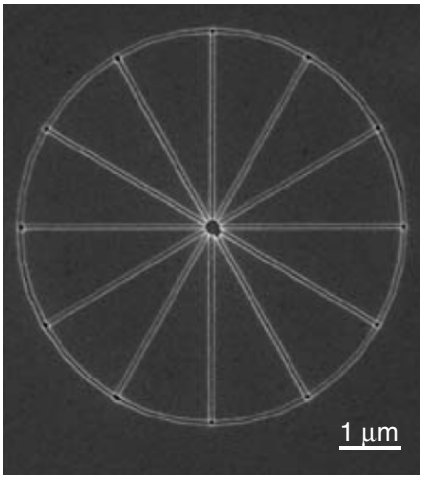

FIGURE 5.7. A wheel pattern that has been written when the beam was out of focus.

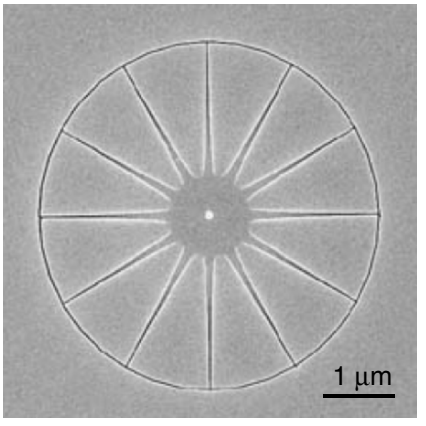

FIGURE 5.8. The wheel pattern written with a high dose.

In general, it is very useful to write an array of a pattern where the applied doses systematically step from a dose that is too low to a dose that is too high. In this way, a new operator can quickly identify the range of resulting structures that are caused by the range of applied doses.

Interference from sources external to the microscope, such as acoustic noise, physical vibrations, or electromagnetic fields, can cause wavy or interrupted lines. In general, the solution is to identify and eliminate the source of the interference or to shield the microscope from the noise. Acoustic noise can be reduced by using acoustic foam on the walls and/or by adding a sound dampening enclosure around the entire column of the microscope. Physical vibration can be minimized by using an air support system for the entire column or simply by adding foam or rubber padding between the column and the floor. Electromagnetic fields that interfere with the beam are often caused by equipment in other rooms or electric lines running through ceilings or floors. These fields can cause the electron beam to deflect at the field frequency, thus causing distortions in the pattern writing. Solutions include moving the microscope to a better location, moving or shielding the source of the interference, installing magnetic shielding (mu-metal) around the column and/or chamber, and installing an active field cancellation system that introduces a magnetic field to cancel the external noise.

5. E-beam Nanolithography Applications in Nanotechnology

Due to its versatility, electron beam lithography is the most common technique used for precise patterning in nanotechnology. Applications include quantum structures, transport mechanisms, solid-state physics, advanced semiconductor and magnetic devices, nanoelectromechanical system (NEMS), and biotechnology. In this section, the applications of electron beam lithography in nanotechnology are demonstrated by four examples in different fields. For each example, the fabrication procedure and device characteristics are discussed.

5.1. Nanotransistors

In the last decade, nanoscale 1D materials and structures have been widely investigated. These structures include semiconductor or metallic nanowires or nanotubes. Electron beam lithography is often involved in either defining the 1D structures directly through top-down nanofabrication [46], forming the catalyst to assist the growth [47], or patterning and wiring the nanowires to nanodevices [48].

As an example, the scanning electron micrograph of a fabricated nanowire Schottky diode is shown in Fig. 5.9. N-type semiconductor ZnO nanowires are synthesized by the vapor phase transport method [49]. A detailed fabrication procedure of this device is shown in Fig. 5.10. The fabrication starts from the Si/SiO_2 substrate. Au electrodes for interconnections are first patterned by photolithography. Then ZnO nanowires are deposited on the substrate by IPA dispersion. In the

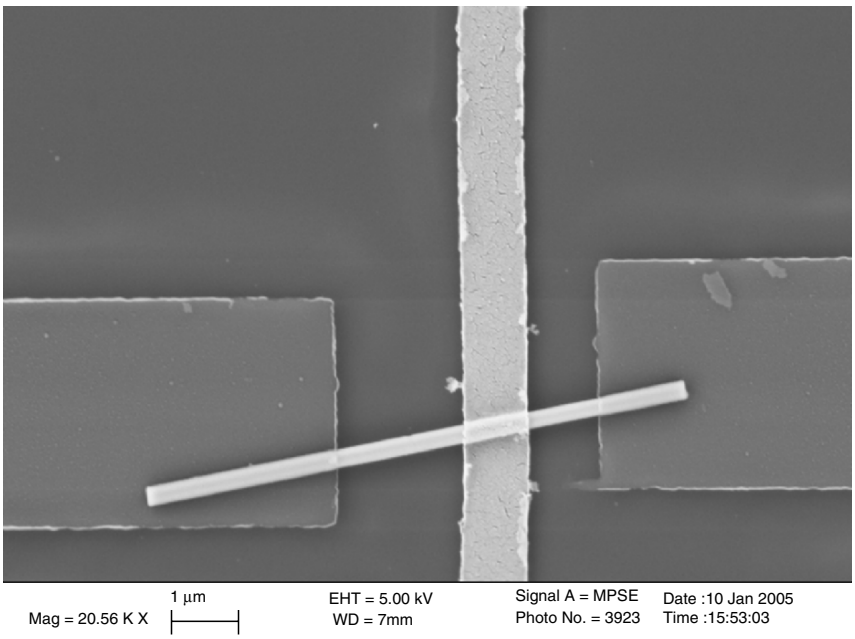

FIGURE 5.9. Scanning electron micrograph of a fabricated ZnO nanowire-based Schottky diode.

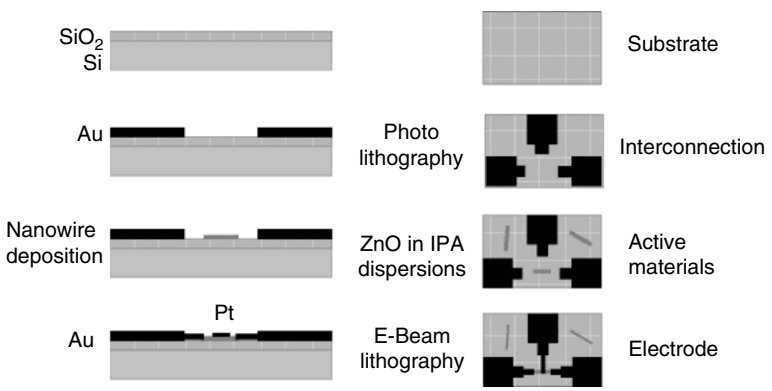

FIGURE 5.10. Step-by-step fabrication procedure of ZnO nanowire Schottky diode.

final step, e-beam lithography is used to connect small leads to the nanowires after aligning to registration marks defined by the photolithography. The Pt electrode deposited over ZnO nanowire forms the Schottky contact with ZnO. The other two electrodes are made by Cr/Au which forms the Ohmic contact with ZnO. Figure 5.11 demonstrates the rectifying characteristics of fabricated Schottky diodes, which shows a rectifying factor around 1.9. Recently, a research

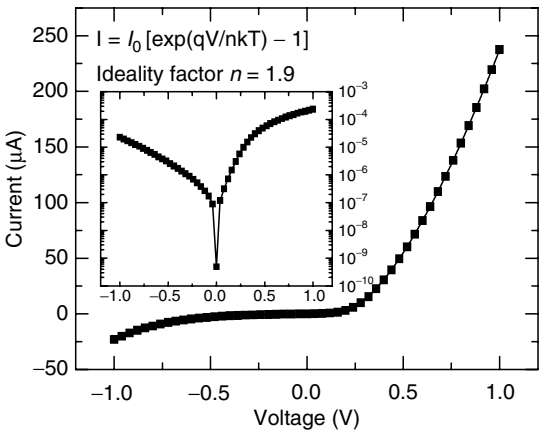

FIGURE 5.11. The I–V characteristics of fabricated ZnO nanowire Schottky diode.

group at Harvard assembled nanowires arrays on patterned electrodes for large size nanoelectronic transistor fabrication [50,51].

5.2. Nanosensors

Semiconducting metal oxides can be used in gas sensing devices and have been extensively studied due to their properties, such as sensitivity to ambient conditions and simplicity in fabrication [52]. Applications in many fields include environmental modeling, automotive applications, air conditioning, and sensor networks. The commercially available gas sensors are made mainly from SnO_2 and In_2O_3 in the form of thick films, porous pellets, or thin films. However, poor long-term stability has prevented wide application of this type sensor. Recent research has been directed toward nanostructured oxides since reactions at grain boundaries and complete depletion of carriers in the grains can strongly modify the materials transport properties [53,54]. Nanowires made of semiconducting metal oxides with a rectangular cross section in a ribbon-like morphology are very promising for sensors because the surface-to-volume ratio is very high [55–57]. Also, the oxide is single crystalline, the faces exposed to the gaseous environmental are always the same, and the small size is likely to produce a complete depletion of carriers inside the nanowires and make the sensor more sensitive.

A ZnO nanowire-based gas sensor is shown in Fig. 5.12a, where the opposite electrodes and comb electrodes are patterned by photolithography and e-beam lithography, respectively. During the second e-beam lithography step, a resist (PMMA) window is opened upon the comb electrodes (Fig. 5.12b). After the deposition of ZnO nanowires from IPA dispersions by the Langmuir-Blodgett technique (Fig. 5.12c), the final liftoff process removes the ZnO nanowires outside the window region along with the PMMA. In this device, the resistance of the nanowires changes with the gas condition and is detected by the I-V characteristics

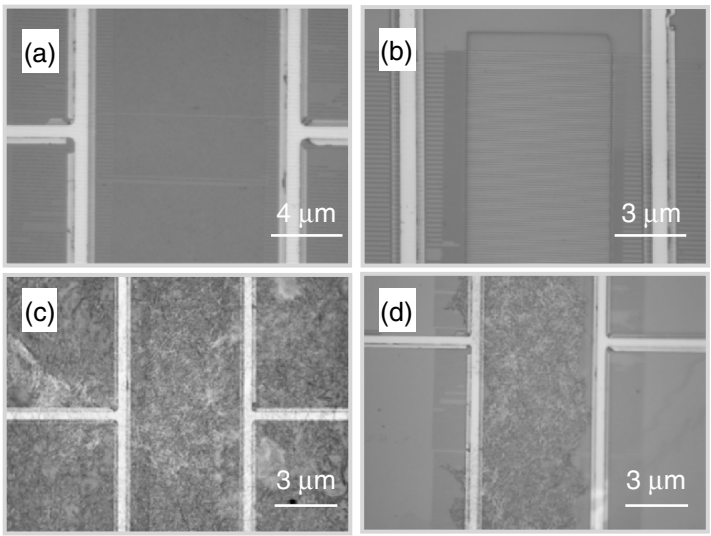

FIGURE 5.12. The optical micrograph of gas sensor: (a) pattern of electrodes; (b) PMMA window between two electrodes; (c) deposition of nanowires by the Langmuir-Blodgett technique; and (d) liftoff process.

between the two electrodes. Due to the small features of the comb electrode structures that are written by e-beam lithography and the usage of nanowires, the surface-to-volume ratio is largely increased, resulting in an improved sensitivity compared to thin film-based gas sensors. Using the electron beam lithography technique, similar nanoscale sensors have also been fabricated with very high resolution, sensitivity, and density [58–60].

5.3. Magnetic Nanodevices

Magnetic nanostructures have become a particularly interesting class of materials for both scientific and technological explorations. To obtain different magnetic nanostructures, e-beam lithography has been used in combination with other lithography processes. One of the main advantages of this approach is its ability to fabricate well-defined shapes for arbitrary elements and also array configurations. A variety of magnetic elements have been achieved such as dots and lines [61,62], rectangles, triangles [63] and pentagons [64], zig-zag lines [65], rings [66] for the study of the magnetization reversal processes. Moreover, this versatility allows the fabrication of nanodevices, such as non-volatile magnetoresistive magnetic random access memories (MRAM) [67] or "quantum" magnetic disks [68,69]. Magnetoelectronics is considered to be one of the most promising approaches for quantum computation [70,71] and universal memory [72] with ultrahigh density.

As an example, Fig. 5.13 shows an SEM micrograph of 200 nm cobalt zigzag wires patterned using electron beam lithography. The wires are connected for a four-point measurement to four gold electrodes which have been fabricated using photolithography. Nanometric wires were used to determine the magnetoresistance of the domain walls in polycrystalline Co. The magnetic switching processes of an array of Co wires are studied by superconducting quantum interference device (SQUID) at the temperature range from 5 to 300 K. Exchange bias was observed in the Co wires at 5 K, which is responsible for the asymmetric behavior of the magnetoresistance, as shown in Fig. 5.14 [65,73].

5.4. Biological Applications

With the assistance of nanolithography, nanoscale devices have also been fabricated for biological applications [74–76]. One example is the biomolecular motor-powered devices developed by Montemagno et al. [74]. In their study, a system is first established to produce a recombinant biomolecular motor. Then biological molecules are positioned on the fabricated nanostructures and then baseline performance data is acquired. Electron beam lithography is used to pattern a metallic (gold, copper, or nickel) array on a 25 mm cover slip. Subsequently, His-tagged 1 μm microspheres are attached to the metallic surface. These motors show promise as mechanical components in hybrid nanoengineered systems. The results demonstrate the ability to engineer chemical

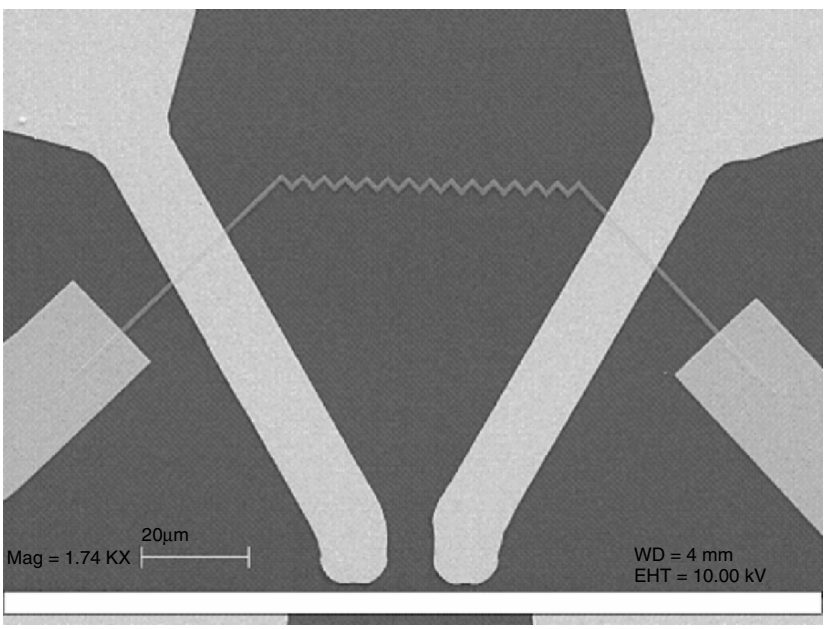

FIGURE 5.13. Co zigzag wires patterned by e-beam lithography.

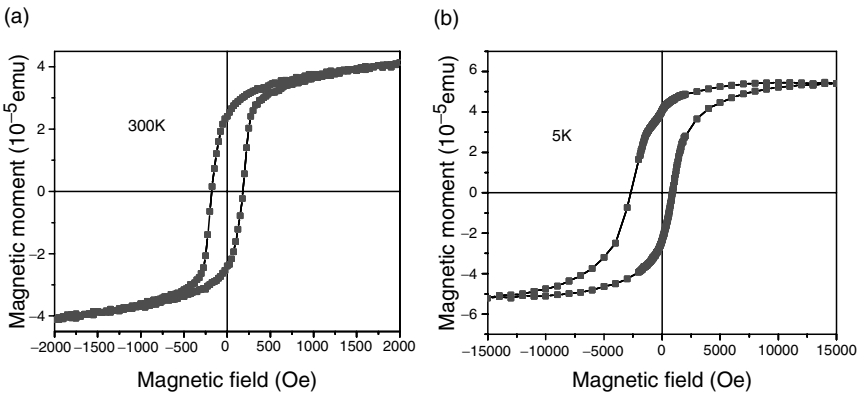

FIGURE 5.14. Field-dependent magnetization of the arrayed Co wires at (a) 5 K and (b) 300 K, respectively.

regulation into a biomolecular motor and represent a critical step toward controlling integrated nanomechanical devices at the single-molecule level.

6. Summary

This chapter introduced technique configurations of electron nanolithography integrated with SEM. Various photo resists and processing preparation were detailed. The step-by-step pattern generation were explicated. Pattern processing and proper writing were also discussed. The applications on nanotransistors, nano-gas sensors, magnetic nanodevices, and biomolecular motor-powered nanodevices have been demonstrated. Electron beam nanolithography shows extreme importance for nanodevice and nanosensor fabrication.

References

1. G. Mollenstedt and R. Speidel, *Phys. Blatter*, 16 (1960) 192.
2. A. N. Broers, in: *Proceedings of the 1st International Conference on Electron and Ion Beam Science and Technology*, R. Bakish (Ed.), Wiley, (1964), pp. 191–204.
3. M. A. McCord and R. F. W. Pease, *J. Vac. Sci. Technol. B*, 4 (1986) 86.
4. A. Majumdar, P. I. Oden, J. P. Carrejo, L. A. Nagahara, J. J. Graham, and J. Alexander, *Appl. Phys. Lett*., 61 (1992) 2293.
5. G. T. A. Kovacs, *Micromachined Transducers Sourcebook*, WCB McGraw-Hill Stanford Univ. (1998).
6. J. Ingino, G. Owen, C. N. Bergulund, R. Browning, and R. F. W. Pease, *J. Vac. Sci. Technol. B*, 12 (1994) 1367.
7. M. Angelopoulos, J. M. Shaw, K. L. Lee, W. S. Huang, M. A. Lecorre, and M. Tissier, *Pol. Eng. Sci*., 32 (1992) 1535.
8. P. Rai-Choudhury, *Handbook of Microlithography, Micromachining, and Microfabrication*, SPIE Optical Engineering Press (1997.)

9. M. Angelopoulos, J. M. Shaw, K. Lee, W. Huang, M. Lecorre, and M. Tissier, *J. Vac. Sci. Technol. B*, 9 (1991) 3428.
10. M. Angelopoulos, N. Partel, J. M. Shaw, N. C. Labianca, and S. A. Rishton, *J. Vac. Sci. Technol. B*, 11 (1993) 2794.
11. P. Romand, A. Weill, J. -P. Panabiere, and A. Prola, *J. Vac. Sci. Technol. B*, 12 (1994) 3550.
12. S. Wolf and R. N. Tauber, "Silicon Process for the VLSI Era," Vol. 1: *Process Technology*, Lattice Press, 2nd edition, November (1999).
13. A. N. Cleland, *Foundations of Nanomechanics*, Springer (2002).
14. A. N. Broers, A. C. F. Hoole, and J. M. Ryan, *Microelectron. Eng*., 32 (1996) 131.
15. M. I. Lutwyche, *Microelectron. Eng*., 17 (1992) 17.
16. I. Kostic, R. Andok, V. Barak, I. Caplovic, A. Konecnikova, L. Matay, P. Hrkut, A. Ritomsky, *J. Mater. Sci.: Mater. Electron*., 14 (2003) 645.
17. I. Zailer, J. E. F. Frost, V. Chabasseur-Molyneux, C. J. B. Ford, M. Pepper, *Semicond. Sci. Technol*., 11 (1996) 1235.
18. M. Khoury and D. K. Ferry, *J. Vac. Sci. Technol. B*, 14(1) (1996) 75–79.
19. A. A. Tseng, K. Chen, C. D. Chen, and K. J. Ma, *IEEE Trans. Electron. Packaging Manuf*., 26 (2003) 141.
20. D. R. Medeiros, A. Aviram, C. R. Guarnieri, W. -S. Huang, R. Kwong, C. K. Magg, A. P. Mahorowala, W. M. Moreau, K. E. Petrillo, and M. Angelopoulos, *IBM J. R&D*, 45 (2001) 639.
21. K. Nakamura, S. L. Shy, C. C. Tuo, and C. C. Huang, *Jpn. J. Appl. Phys*., 33 (1994) 6989.
22. T. Tada, *J. Electrochem. Soc*., 130 (1983) 912.
23. H. Ito, *IBM J. R&D*, 41 (1997) 69.
24. M. Kurihara, T. Segawa, D. Okuno, N. Hayashi, and H. Sano, *Proc. SPIE*, 3412 (1998) 279.
25. T. Segawa, M. Kurihara, S. Sasaki, H. Inomata, N. Hayashi, and H. Sano, *Proc. SPIE*, 3412 (1998) 82.
26. H. Saitoh, T. Soga, S. Kobu, S. Sanki, and M. Hoga, *Proc. SPIE*, 3412 (1998) 269.
27. K. Katoh, K. Kasuya, T. Arai, T. Sakamizu, H. Satoh, H. Saitoh, and M. Hoga, *Proc. SPIE*, 3873 (1999) 577.
28. T. H. P. Chang, D. P. Kern and L. P. Muray, *J. Vac. Sci. Technol. B*, 10 (1992) 2743.
29. M. J. Madou, *Fundamentals of Microfabrication: The Science of Miniaturization*, 2nd edition, CRC Press, 2002.
30. L. E. Ocola, D. Tennant, G. Timp, and A. Novembre, *J. Vac. Sci. Technol. B*, 17 (1999) 3164.
31. M. J. Word, I. Adesida, P. R. Berger, *J. Vac. Sci. Technol. B*, 21 (2003) L12.
32. H. Hamatsu, T. Yamaguchi, M. Nagase, K. Yamasaki, and K. Kurihara, *Microelectron. Eng*., 41/42 (1998) 331.
33. F. C. M. J. M. van Delft, J. P. Weterings, A. K. van Langen-Suurling, H. Romijn, *J. Vac. Sci. Technol. B*, 18 (2000) 3419.
34. S. Matsui, Y. Igaku, H. Ishigaki, J. Fujita, M. Ishida, Y. Ochiai, H. Namatsu, and M. Komuro, *J. Vac. Sci. Technol. B*, 21(2003) 688.
35. I. Junarsa, M. P. Stoykovich, P. F. Nealey, Y. Ma, F. Cerrina, and H. H. Solak, *J. Vac. Sci. Technol. B*, 23 (2005) 138.
36. W. Henschel, Y. M. Georgiev, and H. Kurz, *J. Vac. Sci. Technol. B*, 21 (2003) 2018.
37. G. M. Schmid, L. E. Carpenter II, and J. A. Liddle, *J. Vac. Sci. Technol. B*, 22 (2004) 3497.

38. H. Namatsu, *J. Vac. Sci. Technol. B*, 19 (2001) 2709.
39. J. Fujita, Y. Ohnishi, Y. Ochiai, and S. Matsui, *Appl. Phys. Lett*., 68 (1996) 1297.
40. A. Tilke, M. Vogel, F. Simmel, A. Kriele, R. H. Blick, H. Lorenz, D. A. Wharam, and J. P. Kotthaus, *J. Vac. Sci. Technol. B*, 17 (1999) 1594.
41. M. Aktary, M. O. Jensen, K. L. Westra, M. J. Brett, and M. R. Freeman, *J. Vac. Sci. Technol. B*, 21 (2003) L5.
42. W. Langheinrich, A. Vescan, B. Spangenberg, and H. Beneking, *Microelectron. Eng*., 17 (1992) 287–290.
43. A. N. Broers, A. C. F. Hoole, and J. M. Ryan, *Microelectron. Eng*., 32 (1996) 131.
44. T. Weimann, W. Geyer, P. Hinze, V. Stadler, W. Eck, and A. Golzhauser, *Microelectron. Eng*., 57 (2001) 903.
45. A. N. Broers, A. C. F. Hoole, and J. M. Ryan, *Microelectron. Eng*., 32 (1996) 131.
46. L. Pescini, A. Tilke, R. H. Blick, H. Lorenz, J. P. Kotthaus, W. Eberhardt, and D. Kern, *Nanotechnology*, 10 (1999) 418.
47. N. R. Franklin, Q. Wang, T. W. Tombler, A. Javey, M. Shim, and H. Dai, *Appl. Phys. Lett*., 81 (2002) 913.
48. Y. Huang, X. Duan, Y. Cui, L. J. Lauhon, K. -H. Kim, and C. M. Lieber, *Science*, 294 (2001) 1313.
49. Y. X. Chen, L. J. Campbell, and W. L. Zhou, *J. Cryst. Growth*, 270 (2004) 505.
50. S. Jin, D. Whang, M. C. McAlpine, R. S. Friedman, Y. Wu, and C. M. Lieber, *Nano Lett*., 4 (2004) 915.
51. D. Whang, S. Jin, and C. M. Leiber, *Nano Lett*., 3 (2003) 951.
52. N. Barsan, M. Schweizer-Berberich, and W. Gëpel, *Fresenius J. Anal. Vol*., 365 (1999) 287.
53. W. Gëpel, *Sens. Actuators A*, 56 (1996) 83.
54. M. Ferroni, V. Guidi, G. Martinelli, E. Comini, G. Sberveglieri, D. Boscarino, and G. Della Mea, *J. Appl. Phys*., 88 (2000) 1097.
55. E. Comini, G. Faglia, G. Sberveglieri, Z. Pan, and Z. L. Wang, *Appl. Phys. Lett*., 81 (2003) 1869.
56. D. Zhang, C. Li, S. Han, X. Liu, T. Tang, W. Jin, and C. Zhou, *Appl. Phys. Lett*., 82 (2003) 112.
57. C. Li, D. Zhang, X. Liu, S. Han, J. Han, and C. Zhou, *Appl. Phys. Lett*., 82 (2003) 1613.
58. T. Toriyama and S. Sugiyama, *Sens. Actuators A Phys*., 108 (2003) 244.
59. B. Ilic, H. G. Craighead, S. Krylov, W. Senaratne, C. Ober, and P. Neuzil, *J. Appl. Phys*., 95 (2004) 3694.
60. F. Patolsky and C. M. Lieber, *Mater. Today*, 4 (2005) 20.
61. J. F. Smyth, S. Schltz, D. Kern, H. Schmid, and D. Yee, *J. Appl. Phys*., 63 (1988) 4237.
62. J. I. Martin, J. L. Vicent, J. V. Anguita, and F. Briones, *J. Magn. Magn. Mater*., 203 (1999) 156.
63. B. Khamsehpour, C. D. W. Wilkinson, J. N. Chapman, and A. B. Johnston, *J. Vac. Sci. Technol. B*, 18 (2000) 16.
64. R. P. Cowburn, *J. Phys. D*, 33 (2000) R1.
65. T. Taniyama, I. Nakatani, T. Namikawa, and Y. Yamazaki, *Phys. Rev. Lett*., 82 (1999) 2780.
66. J. Rothman, M. Klaui, L. Lopez-Diaz, C. A. F. Vaz, A. Bleloch, J. A. C. Bland, Z. Cui, and R. Speaks, *Phys. Rev. Lett*., 86 (2001) 1098.
67. K. Nordquist, S. Pandharkar, M. Durlam, D. Resnick, S. Teherani, D. Mancini, T. Zhu, and J. Shi, *J. Vac. Sci. Technol. B*, 15 (1997) 2274.

68. S. Y. Chou and P. R. Krauss, *J. Magn. Magn. Mater*., 155 (1996) 151.
69. C. Haginoya, K. Koike, Y. Hirayama, J. Yamamoto, M. Ishibashi, O. Kitakami, and Y. Shimada, *Appl. Phys. Lett*., 75 (1999) 3159.
70. G. A. Prinz, *Science*, 282 (1998) 1660.
71. S. D. Sarma, *Am. Sci*., 89 (2001) 516.
72. S. A. Wolf, D. D. Awschalom, R. A. Buhrman, J. M. Daughton, S. von Molnar, M. L. Roukes, A. Y. Chtchelkanova, and D. M. Treger, *Science*, 294 (2001) 1488.
73. C. Chen, M. H. Yu, Mo. Zhu, and W. L. Zhou, unpublished work.
74. C. Montemagno and G. Bachand, *Nanotechnology*, 10 (1999) 225.
75. R. H. Austin, J. O. Tegenfeldt, H. Cao, S. Y. Chou, E. C. Cox, *IEEE Trans. Nanotechnol*., 1 (2002) 12.
76. R. Bunk, J. Klinth, J. Rosengren, I. Nicholls, S. Tagerud, P. Omling, A. Mansson, and L. Montelius, *Microelectron. Eng*., 67 (2003) 899.